

Thermoelectric Oxide Materials For Electric Power Generation

Kunihito Koumoto

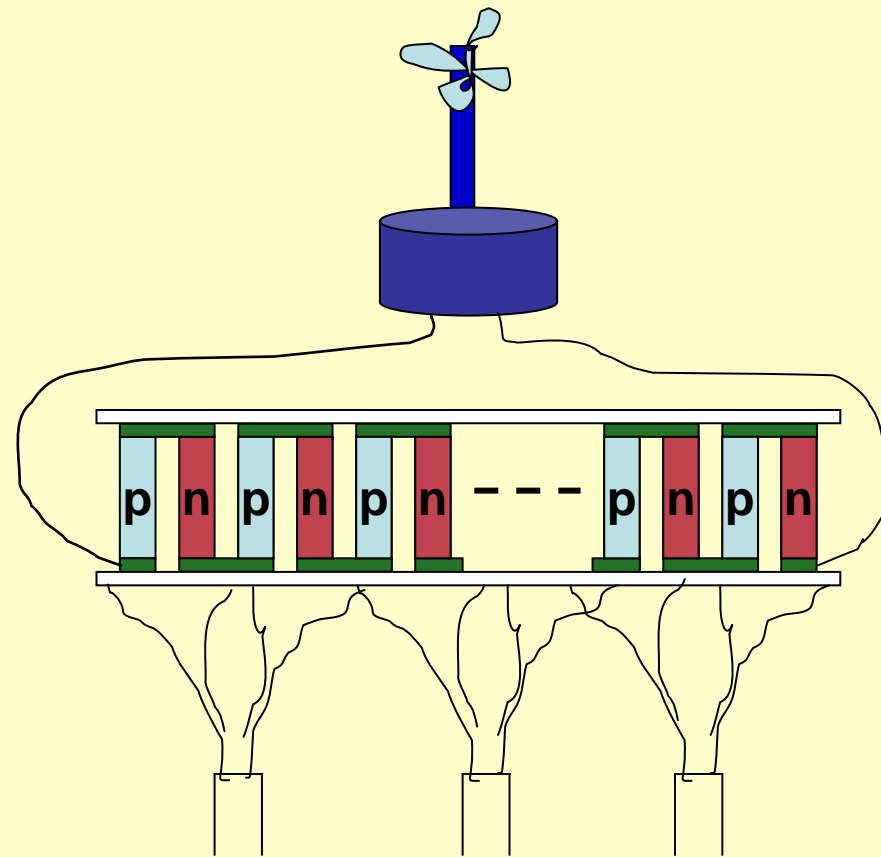
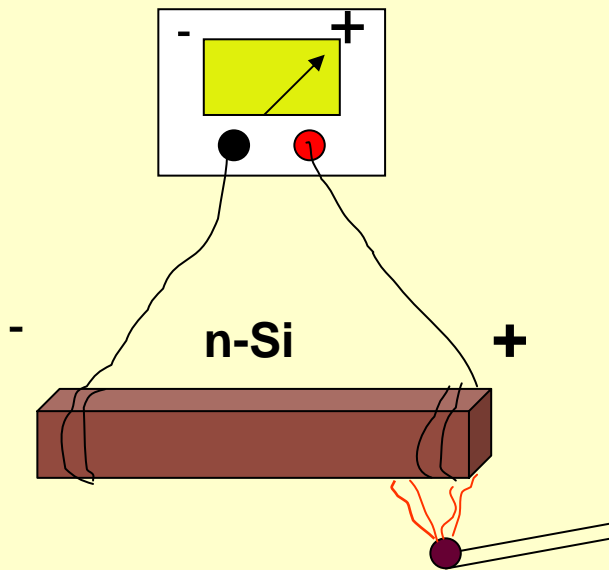
Nagoya University, Graduate School of Engineering
CREST, Japan Science and Technology Agency

1. *Thermoelectric Energy Conversion*
2. *Oxide Superlattices*
3. *Thin Film TE Devices*

Seebeck Effect

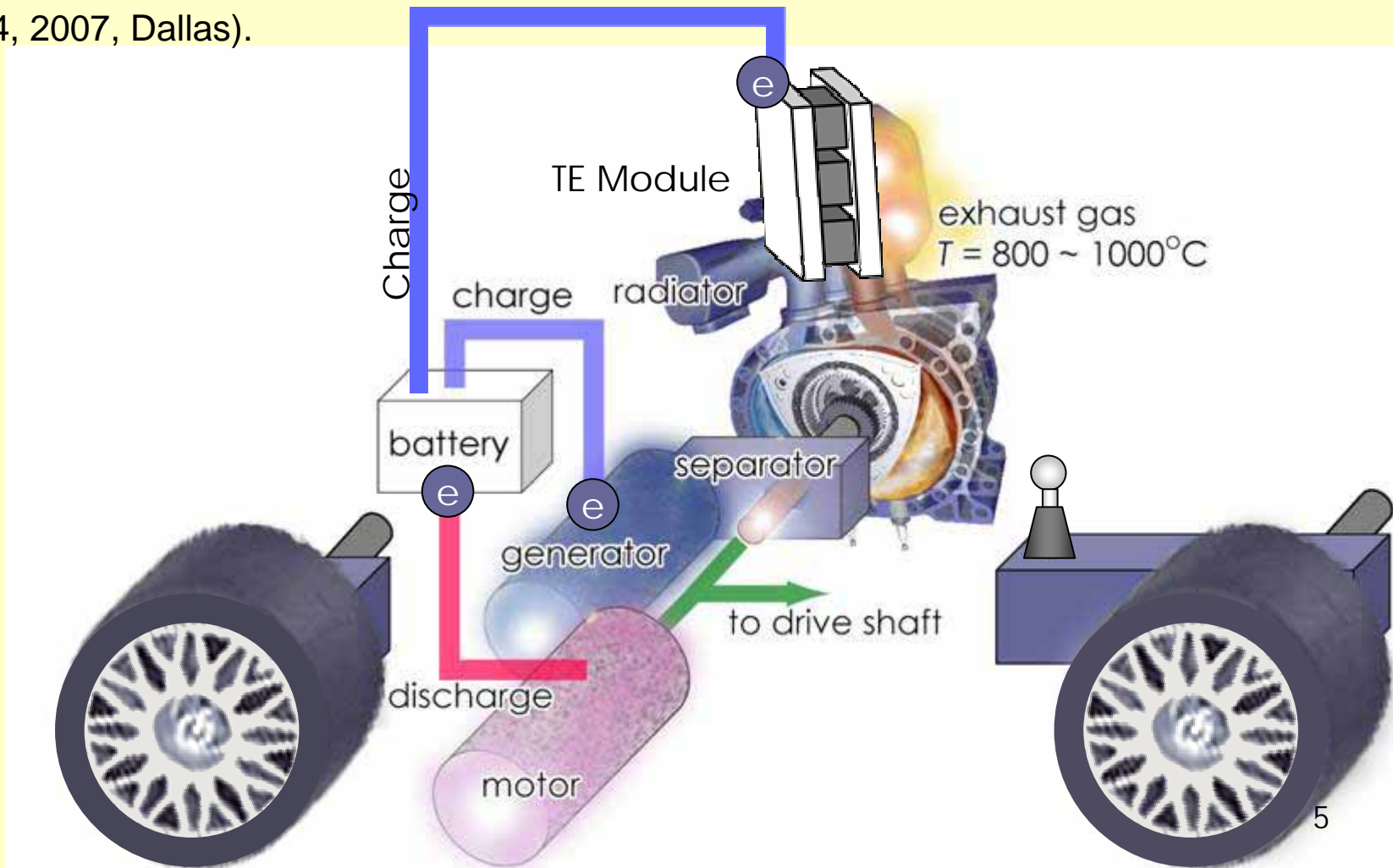
Power generation by a TE module

Voltage meter



TE Technology for Waste Heat Recovery

"Even at the current efficiencies of thermoelectric devices, 7 to 8 percent, more than 1.5 billion gallons of diesel could be saved each year in the U.S. if thermoelectric generators were used on the exhaust of heavy trucks. That translates into billions of dollars saved." by Prof. T. Tritt (NanoTX'07 Conference, Oct. 2-4, 2007, Dallas).



Problems of the Conventional TE Materials

Conventional materials: Bi_2Te_3 , Sb_2Te_3 , $\text{PbTe-Ag}_2\text{Te}$,
 $(\text{Bi},\text{Sb})_2\text{Te}_3$, CoSb_3 , etc.

1. Low Heat Resistance & Oxidation Resistance

Melting point of Bi_2Te_3 : 580

Comparison : Automobile exhaust gas 800 ~1000

2. Limitation of resources

Very small Clarke Numbers

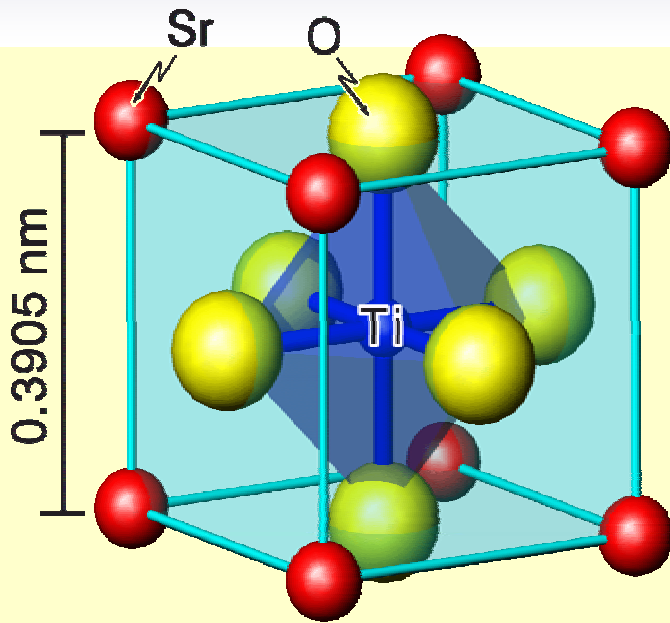
$\text{Bi} : 2 \times 10^{-5} \%$, $\text{Sb} : 5 \times 10^{-5} \%$, $\text{Pb} : 1.5 \times 10^{-3} \%$, $\text{Te} : 2 \times 10^{-7} \%$

Ref. $\text{Pt} : 5 \times 10^{-7} \%$

3. High toxicity

***Oxide TE Materials are highly wanted
for power generation in air atmosphere !***

SrTiO₃ : Good Candidate

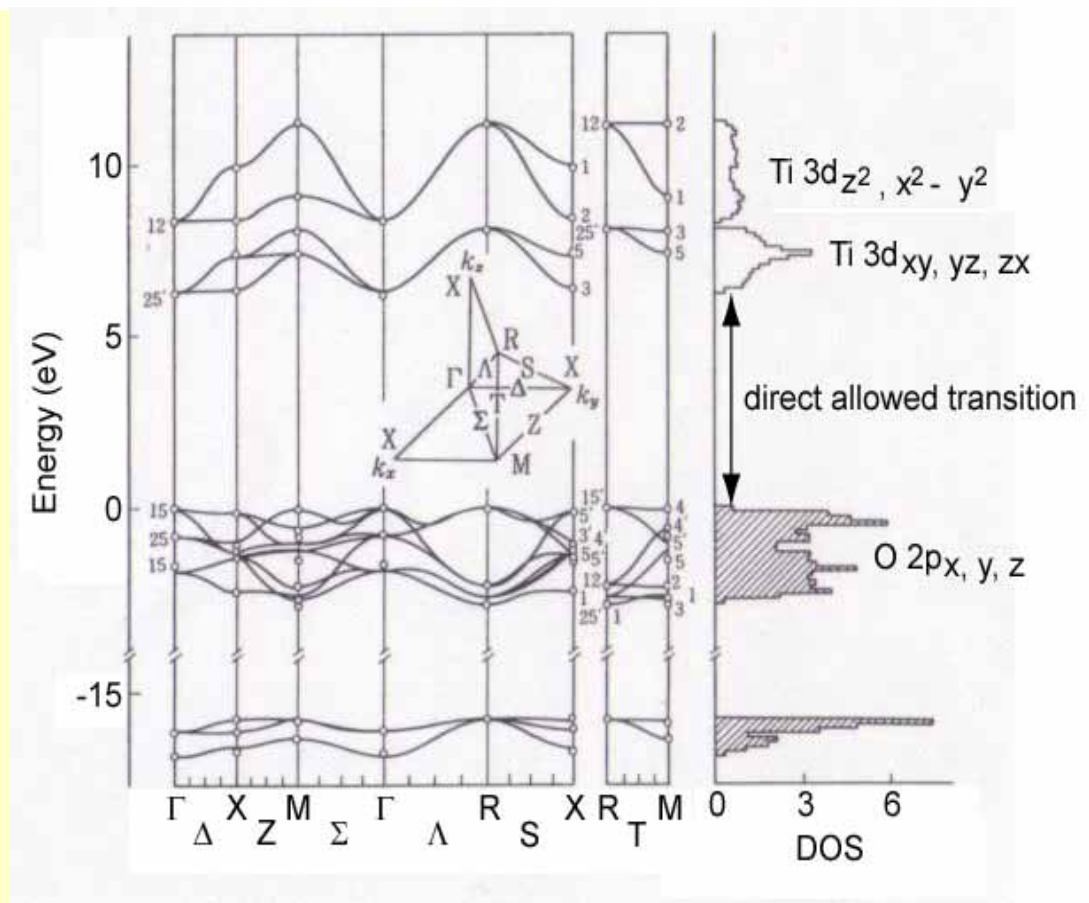


SrTiO₃ Single X'tal

$$E_g = 3.0 \sim 3.2 \text{ eV}$$

$$m^*_{\text{STO}} = \sim 3 \text{--} 10 m_0$$

(Frederikse *et al.* PR, 1964;
Tokura *et al.* PRB, 2001)



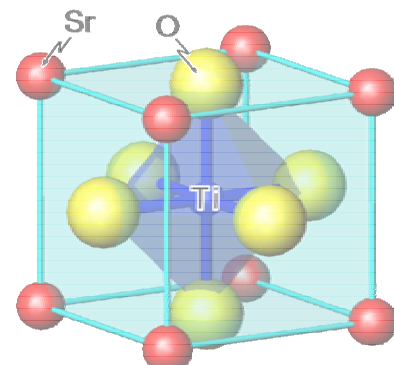
(L. F. Mattheiss, *et al* PRB., 1972)

Strategy

Cubic perovskite-type SrTiO_3

- Excellent controllability of electrical conductivity by doping
→ **High electrical conductivity, σ**
- Large carrier effective mass ($m^* = 6\text{-}11 m_0$)
→ **Large Seebeck coefficient, $|S|$**
- The largest ZT among n-type TE oxides
→ **$ZT = 0.37 @ 1000K$ ($\text{SrTi}_{0.8}\text{Nb}_{0.2}\text{O}_3$)**

[S. Ohta et al. *Appl. Phys. Lett.* **87** (2005)]



Improvement in ZT by reduction of thermal conductivity (κ)
and/or further enhancement of power factor ($S^2 T$)

$$ZT = S^2 T / \kappa$$

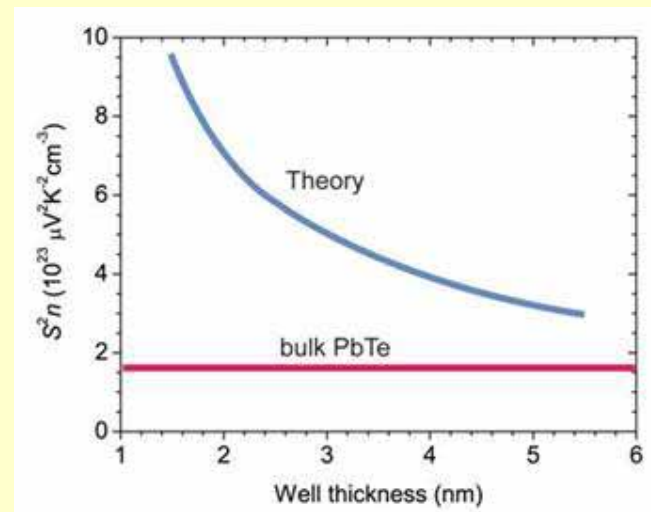
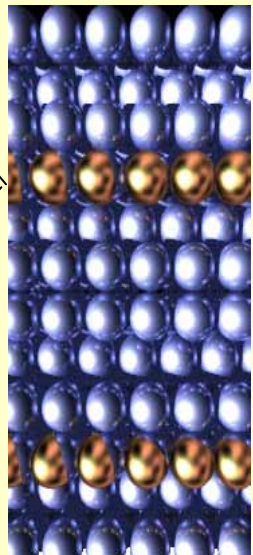
Superlattice

Artificial Superlattice

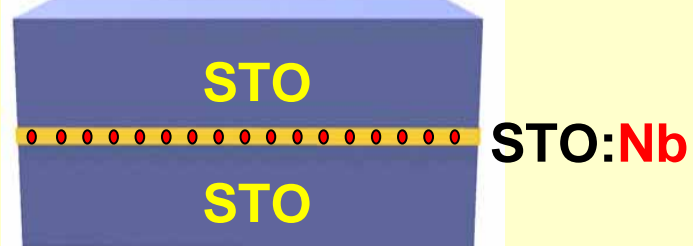
“If electrons were confined in a very narrow space,
you would get enhanced thermopower!”

Hicks and Dresselhaus, Phys. Rev. B **47**, 12727 (1993).

Thin layer with confined
electrons

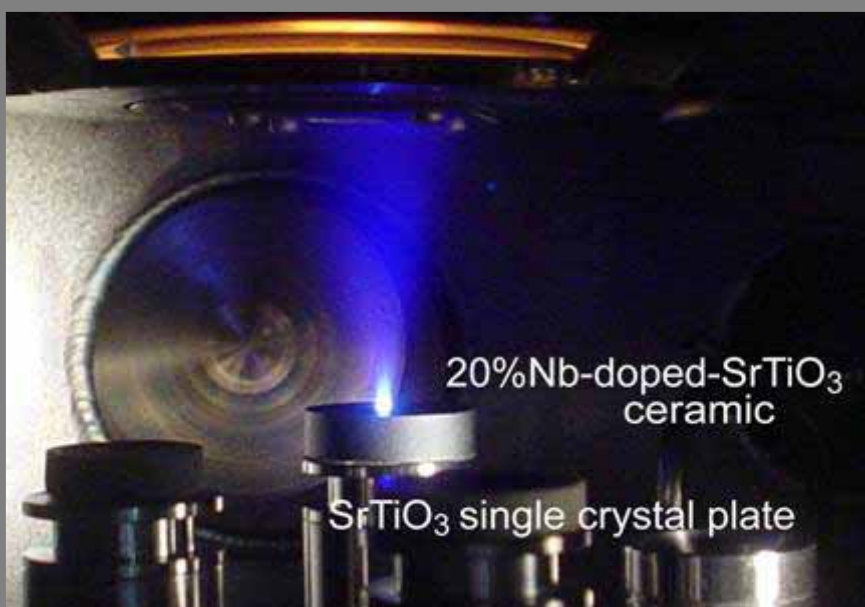
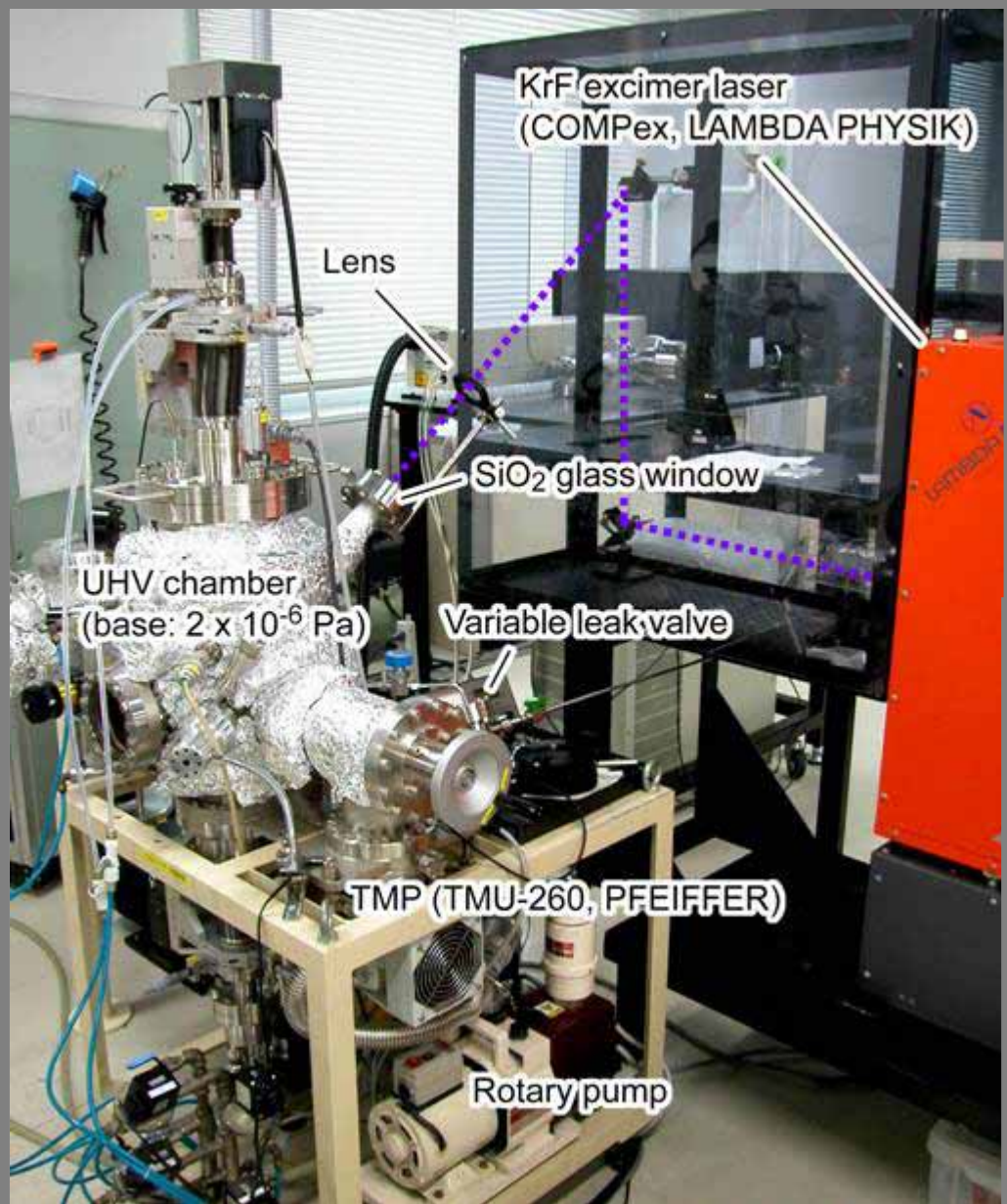


STO/STO:Nb SL



STO:Nb

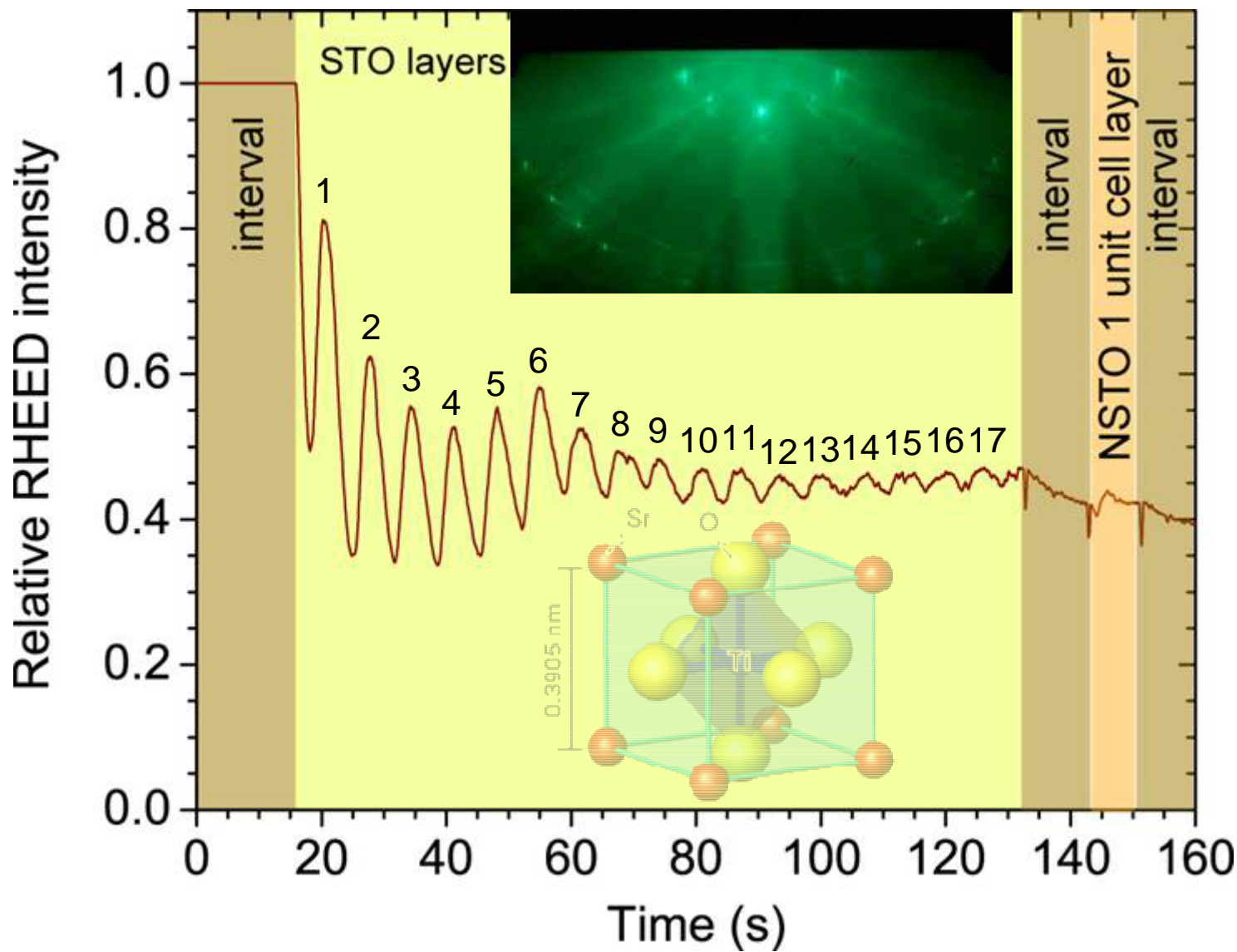
Fabrication of SrTiO₃/Nb:SrTiO₃ superlattice



Growth condition

Substrate	(100)-LaAlO ₃
Growth temp.	900°C
Oxygen pressure	3×10^{-3} Pa
Laser energy density	$\sim 1 \text{ Jcm}^{-2}\text{pulse}^{-1}$
Repetition rate	10 Hz
Growth rate	$\sim 50 \text{ pm s}^{-1}$

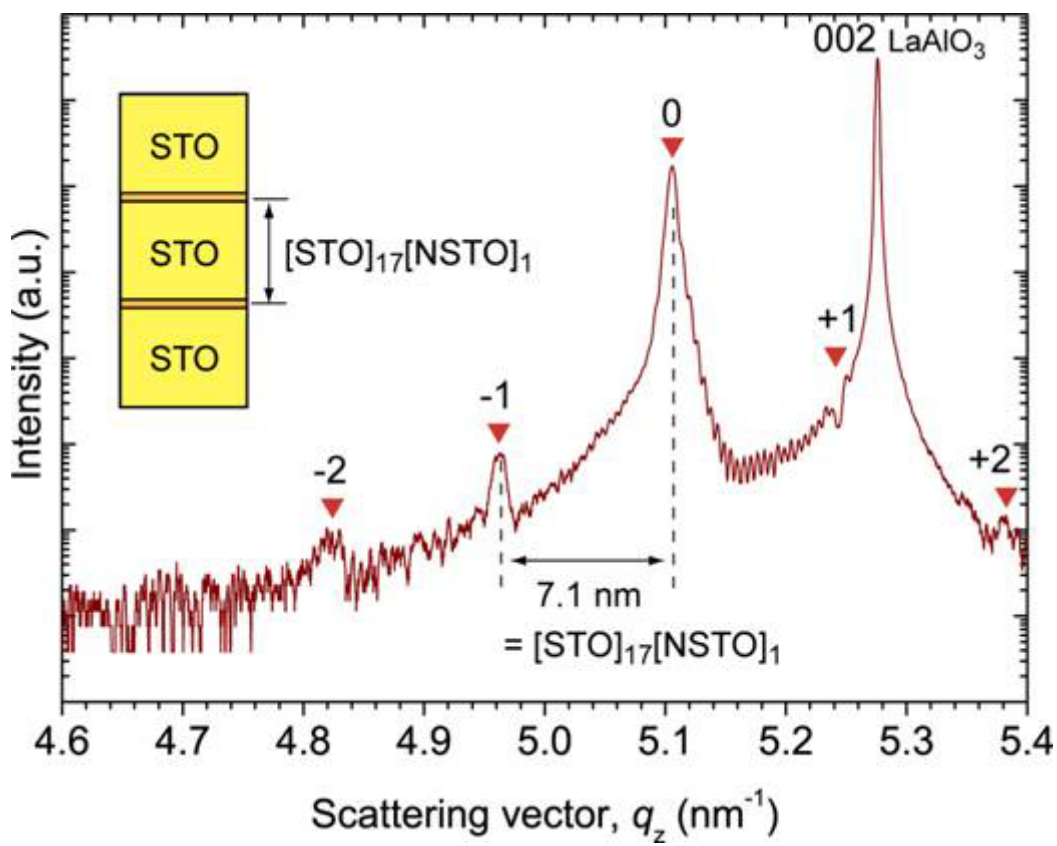
RHEED intensity oscillation



XRD & AFM

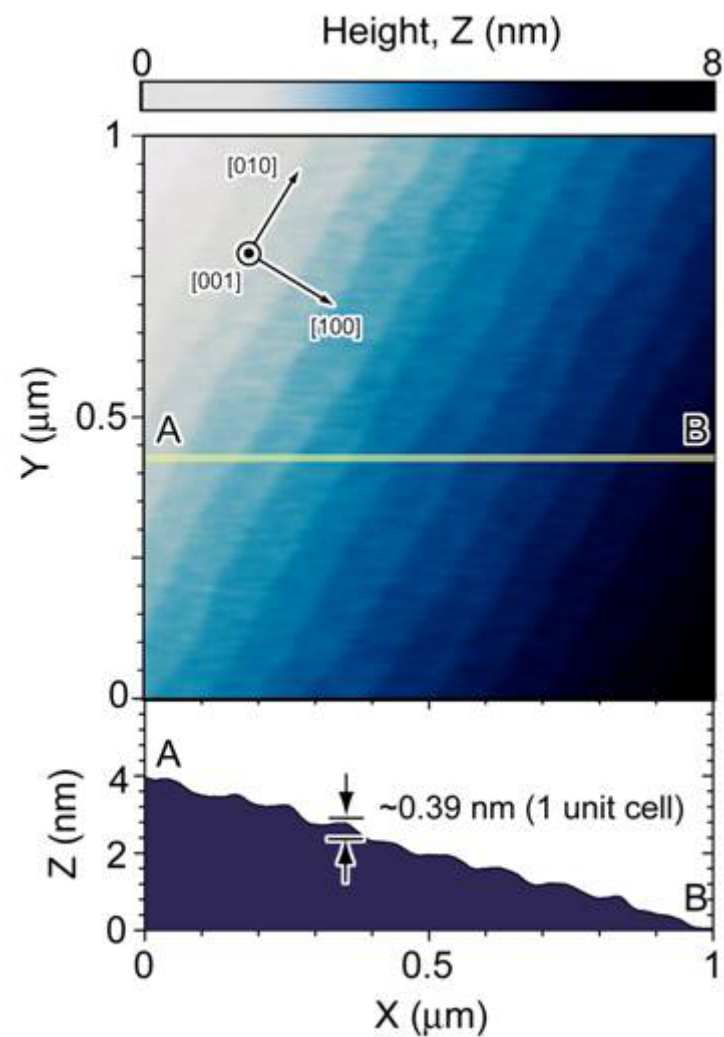
Out-of-plane XRD pattern

*Satellite peaks due to superlattice
are clearly seen*



Topographic AFM image

Frank Van der Merwe (2D) growth

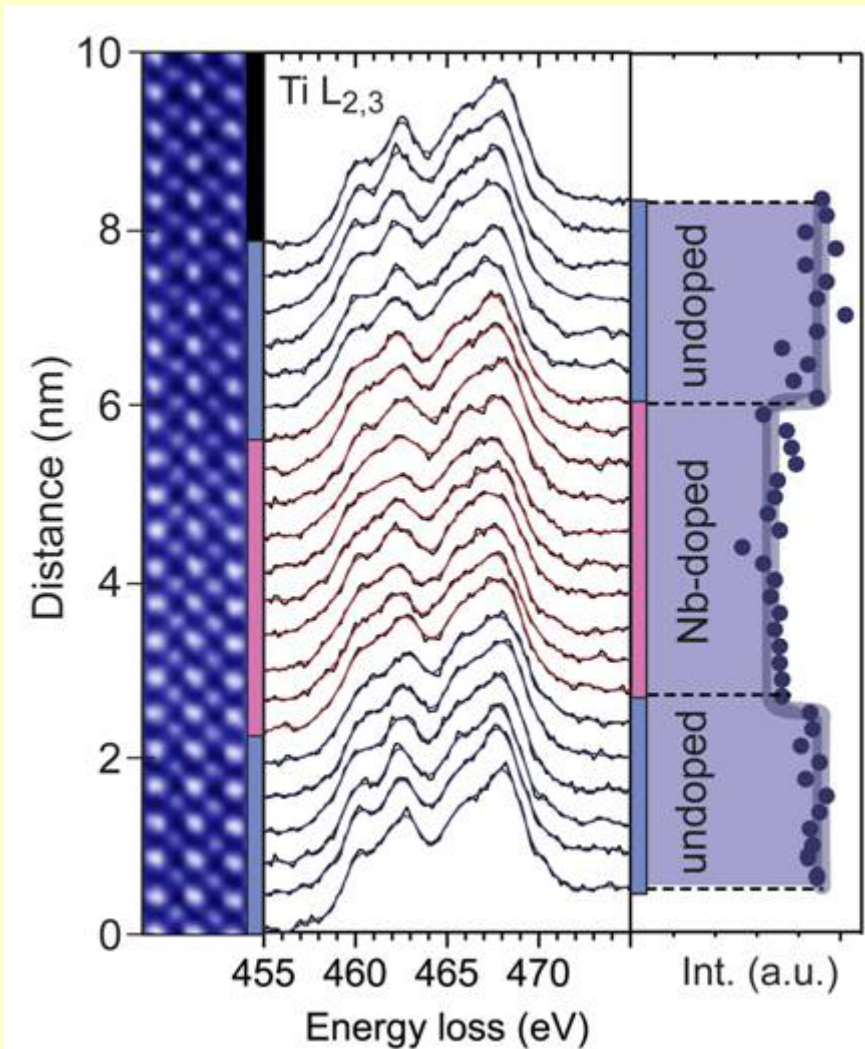


HAADEF-STEM & HREELS

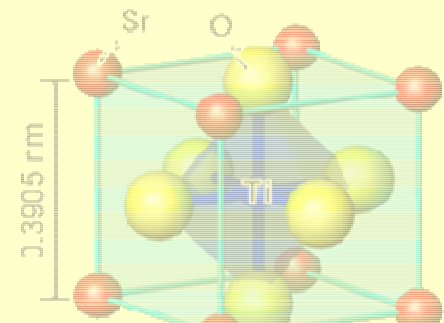
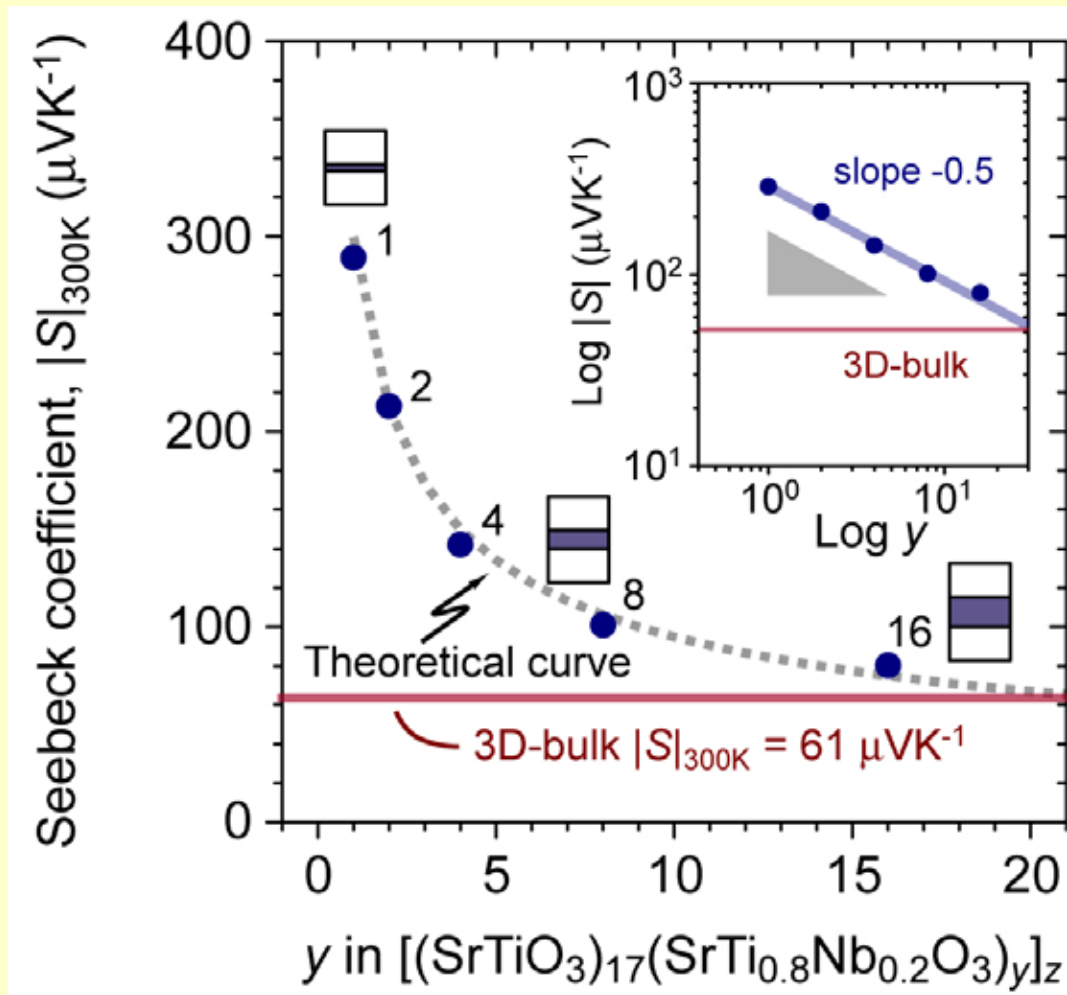


HREELS

Diffusion of dopant Nb did not take place!

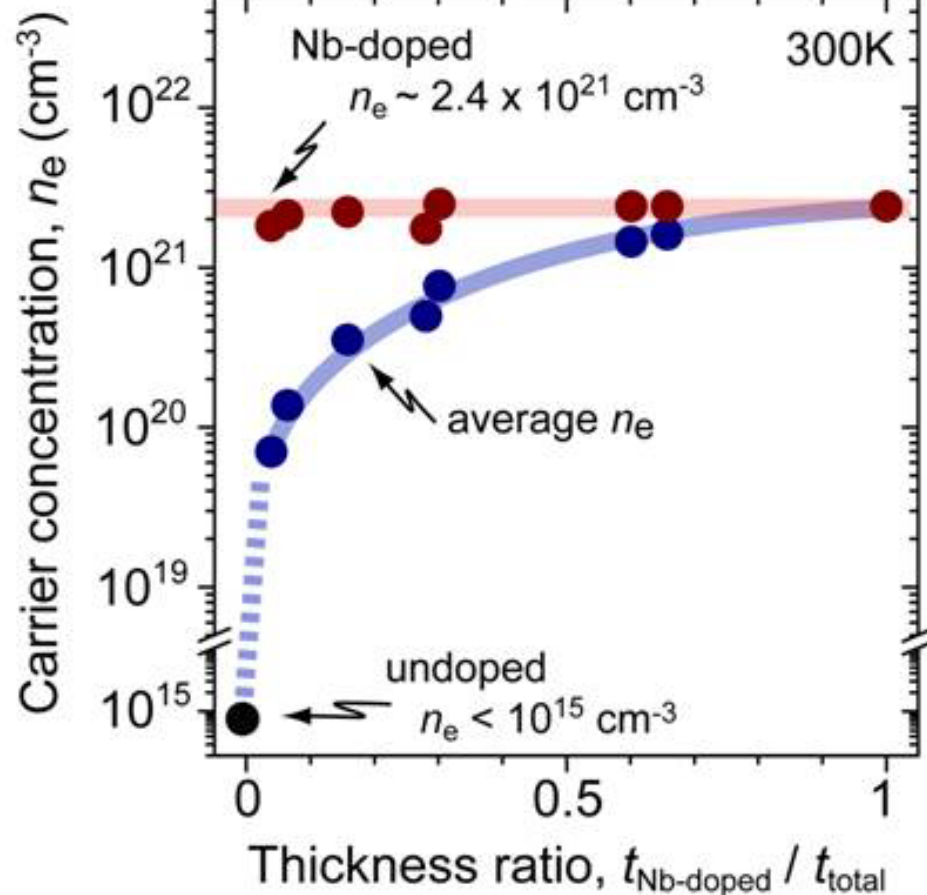


Seebeck coefficient vs. well thickness



H. Ohta et al.,
Nature Mater., 6, 129 (2007)

Electrical Conductivity



Nb-doped STO Layer

Electrical conductivity

$$\sigma = 2.3 \times 10^3 \text{ S cm}^{-1} \text{ at } 300\text{K}$$

Hall mobility

$$\mu_{\text{Hall}} \sim 6 \text{ cm}^2 \text{V}^{-1} \text{s}^{-1} \text{ at } 300\text{K}$$

Carrier concentration

$$n_e = 2.4 \times 10^{21} \text{ cm}^{-3} \text{ at } 300\text{K}$$

H. Ohta et al.,
Nature Mater., 6, 129 (2007)

Thermoelectric figure of merit, ZT

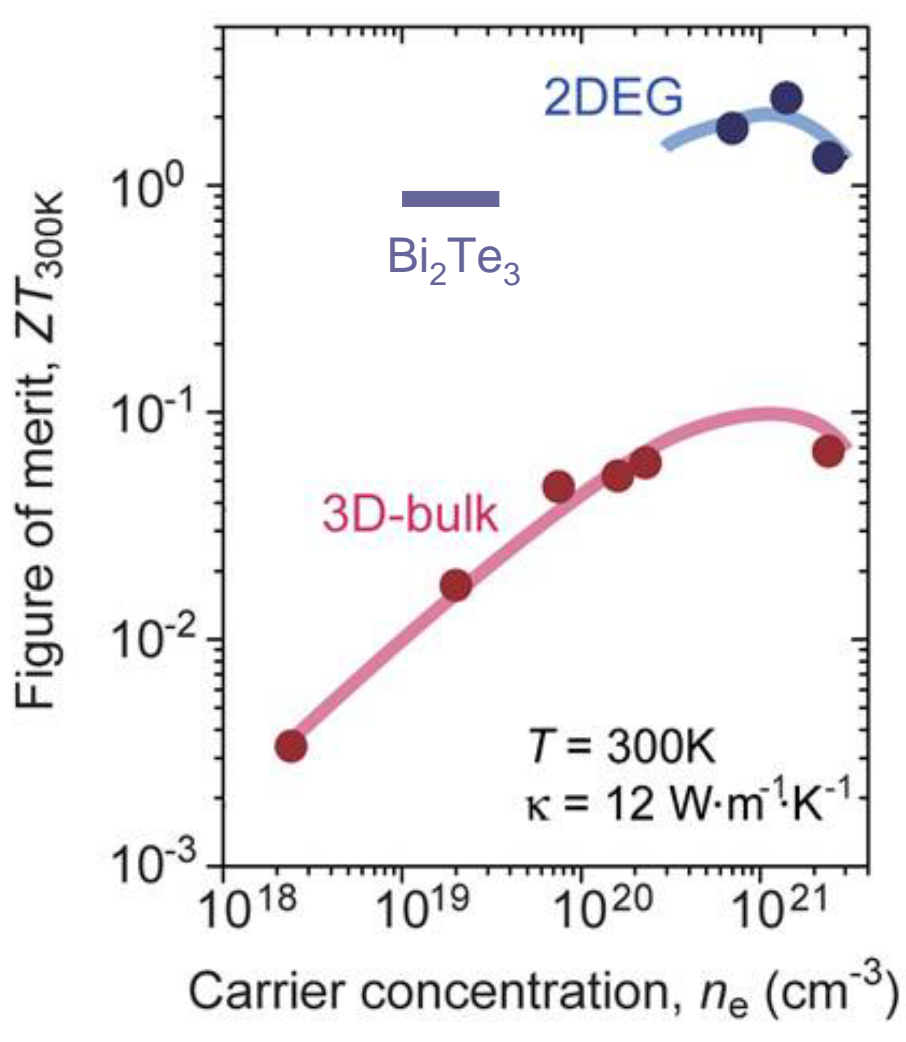


Figure of merit ZT

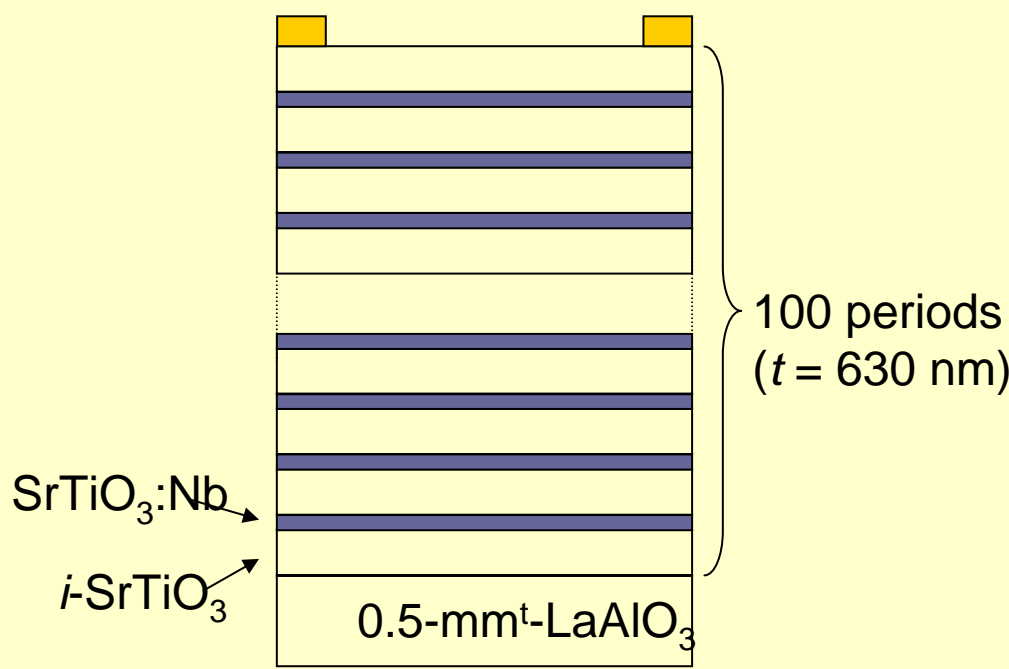
*The optimized ZT value in the **2DEG** system reaches $ZT_{300K}(2DEG) = 2.4$, which is 24 times larger than that of the corresponding 3D-bulk SrTiO_3*

Cf: $\text{Bi}_2\text{Te}_3/\text{Sb}_2\text{Te}_3$ SL
 $ZT_{300K} = 2.4$

(Venkatasubramanian et al.,
Nature, 2001)

H. Ohta et al.,
Nature Mater., 6, 129 (2007)

Direct Heating Test : STO/STO:Nb Superlattice



50 mV @ T=140 K



Cf: Bi₂Te₃

1 unit cell $\text{SrTiO}_3:\text{Nb}$

Carrier electron concentration, $n_e = 4 \times 10^{21} \text{ cm}^{-3}$

Hall mobility, $\mu_{\text{Hall}300\text{K}} = 5 \text{ cm}^2 \cdot \text{V}^{-1} \cdot \text{s}^{-1}$

Electrical conductivity, $\sigma_{300\text{K}} = 3,200 \text{ S} \cdot \text{cm}^{-1}$

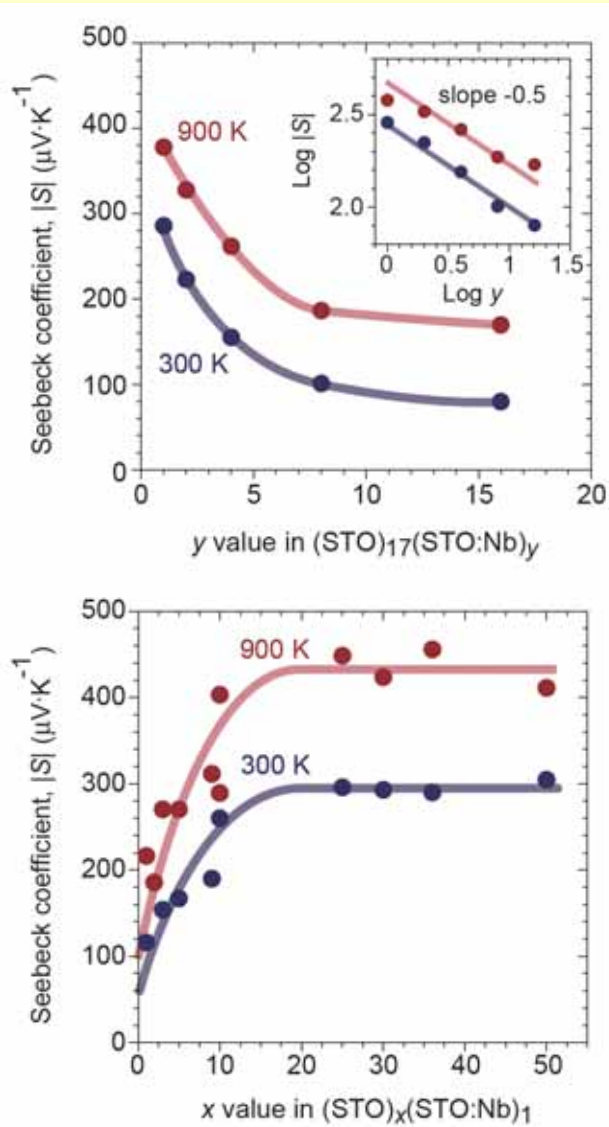
Seebeck coefficient, $|S|_{300\text{K}} = 350 \mu\text{V} \cdot \text{K}^{-1}$

$$\sigma_{300\text{K}} = 1,200 \text{ Scm}^{-1}$$

$$S_{300\text{K}} = 200 \mu\text{V K}^{-1}$$

28 mV @ T=140 K

High-Temp. Characteristics of STO/STO:Nb SL



TE Conversion Efficiency of Superlattice

$$T_c = 300 \text{ K}, T_h = 900 \text{ K}$$

ZT = 2.4 @ 300 K, ZT = 1.4 @ 900 K

$ZT(\text{average}) \sim 1.9$ is assumed.

$$= \frac{W_{out}}{Q_{in}} = \frac{T_h - T_c}{T_h} \frac{(1 + ZT_m)^{1/2} - 1}{(1 + ZT_m)^{1/2} + \frac{T_c}{T_h}}$$

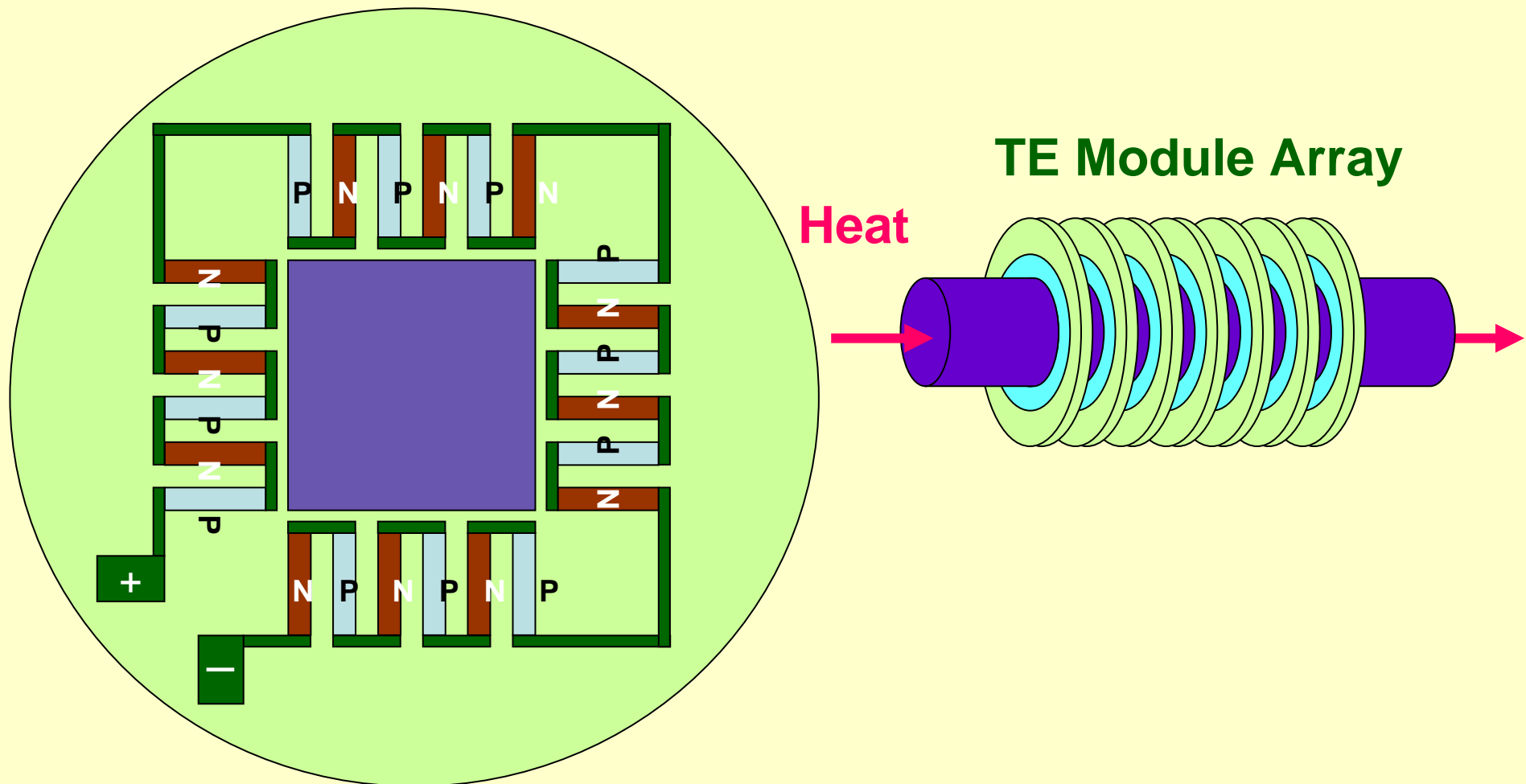
TE.C.E $\sim 22\%$

Cf: Bi_2Te_3 $T_c = 300 \text{ K}, T_h = 500 \text{ K}$
 $ZT(\text{average}) \sim 1.0$ $\sim 8.2\%$

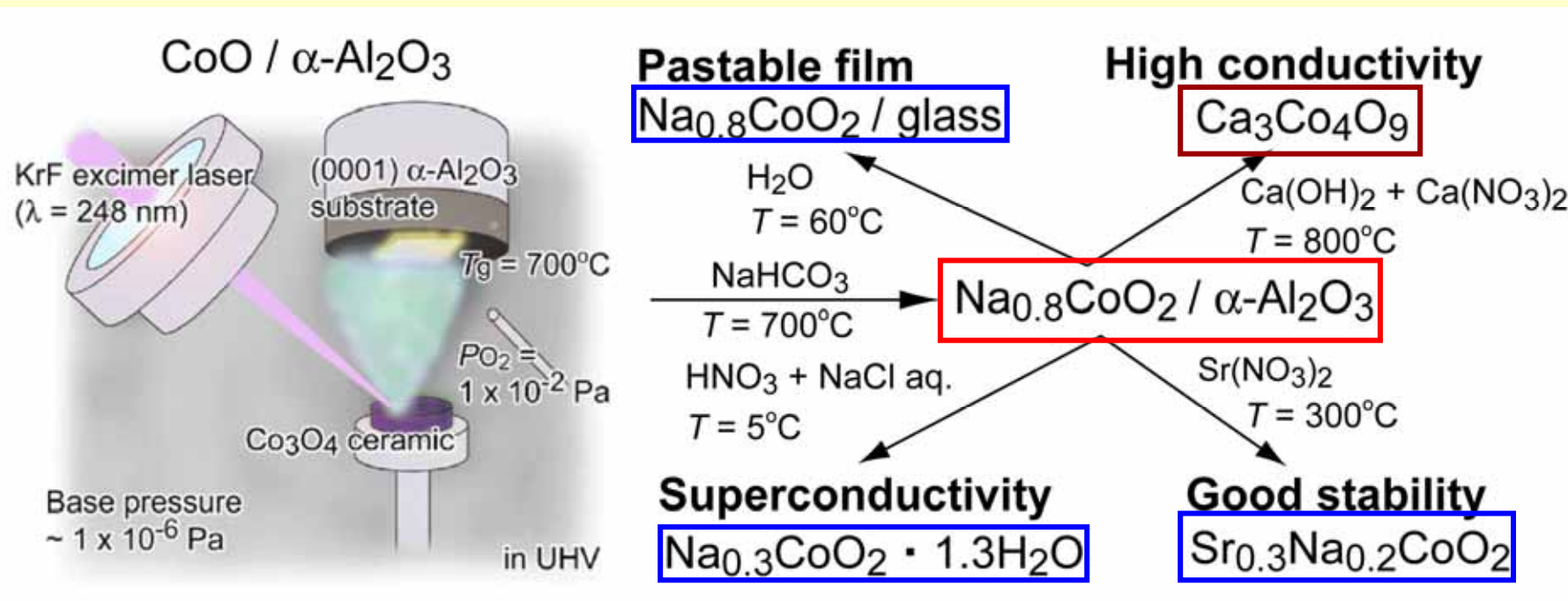
Design Concept for TE Thin Film Module

N-type TE element : STO/STO:Nb Superlattices

P-type TE element : $\text{Ca}_3\text{Co}_4\text{O}_9$ Thin Films



P-type Layered Cobalt Oxide for TE Thin Film Module



H. Ohta et al., *Cryst. Growth & Design*, **5**, 215-218 (2005).

K. Sugiura et al., *Appl. Phys. Lett.*, **88**, 082109 (2006).

K. Sugiura et al., *Inorg. Chem.*, **45**, 1894-96 (2006).

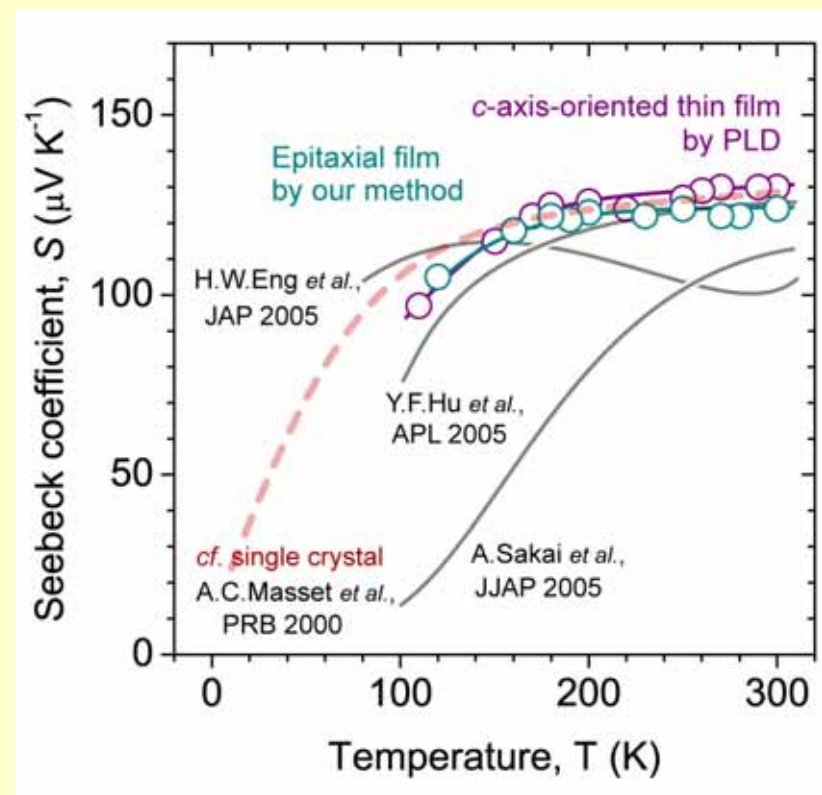
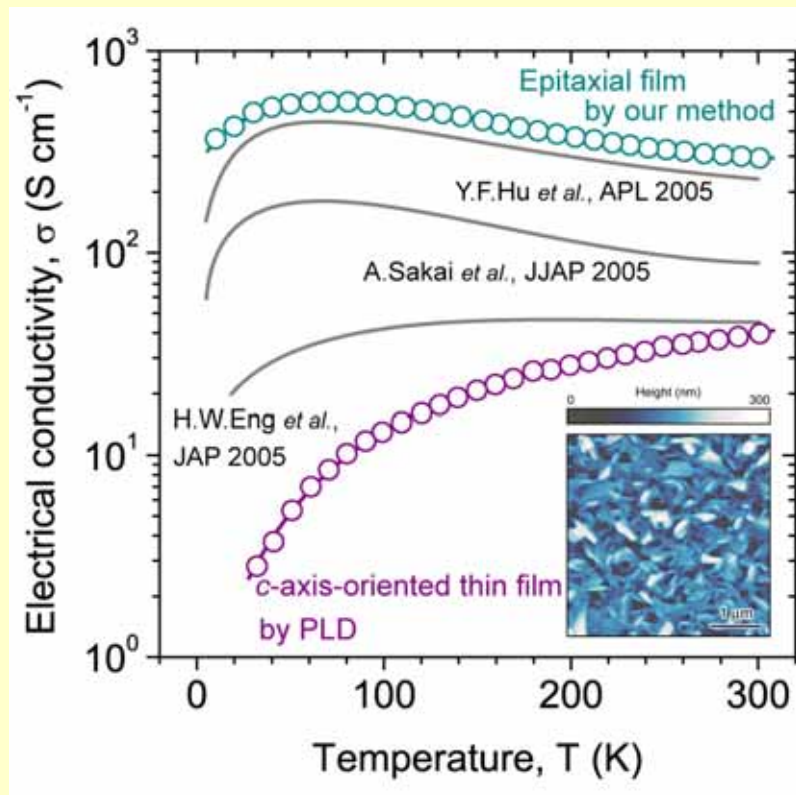
K. Sugiura et al., *Appl. Phys. Lett.*, **89**, 032111 (2006).

H. Ohta et al., *Adv. Mater.*, **18**, 1649-1452 (2006).

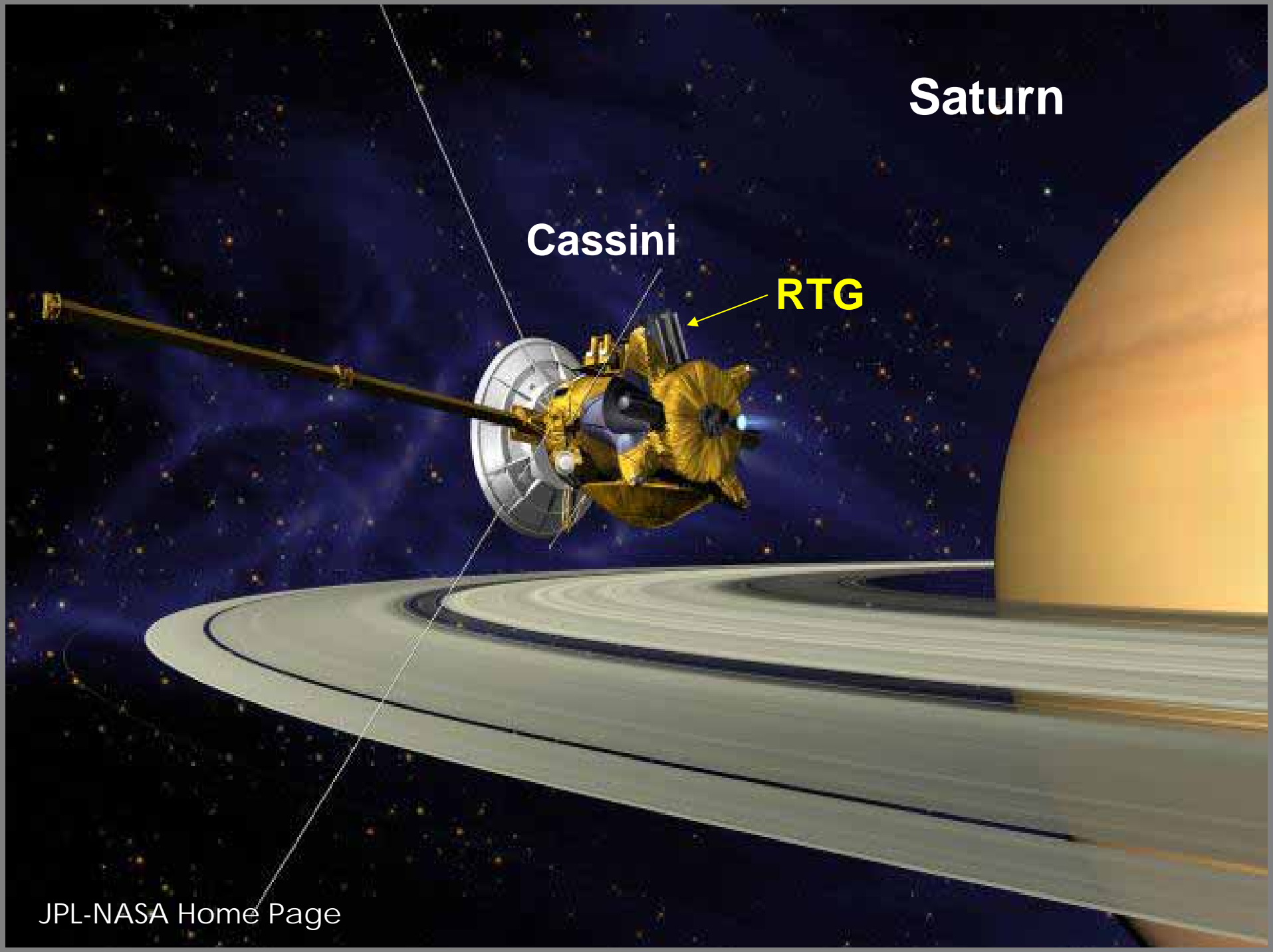
K. Sugiura et al., *Int. J. Adv. Ceram. Technol.*, **4**, 308-317 (2007).

High TE Performance of $\text{Ca}_3\text{Co}_4\text{O}_9$ Thin Film

K. Sugiura et al., *Appl. Phys. Lett.*, **89**, 032111 (2006).



	CCO/film	$\text{Bi}_2\text{Te}_3/\text{bulk}$	STO/SL
PF (S^2) @300K($\times 10^{-3}$)	0.5	4.8	39

A detailed illustration of the Cassini-Huygen probe in space. The probe is shown from a three-quarter perspective, featuring its white cylindrical body, gold-colored thermal insulation panels, and various scientific instruments. It is positioned in front of the large, light-orange planet Saturn, which dominates the right side of the frame. One of Saturn's prominent rings is visible in the lower-left foreground. A long, thin, gold-colored solar panel extends to the left. Several lines connect labels to specific parts of the probe: a line labeled "Cassini" points to the main body, another line labeled "RTG" points to one of the gold panels, and a third line points to the ring system.

Saturn

Cassini

RTG

